Research Article

Saira Akhtar, Kashif Barkat*, Nariman Shahid, Irfan Anjum, Syed Faisal Badshah, Maryam Shabbir, Samir Ibenmoussa, Yousef A. Bin Jardan, Mohammed Bourhia, Ahmad Mohammad Salamatullah, Musaab Dauelbait*

Fabrication of β-cyclodextrin-based microgels for enhancing solubility of Terbinafine: An *in-vitro* and *in-vivo* toxicological evaluation

https://doi.org/10.1515/chem-2024-0084
received April 3, 2024; accepted August 2, 2024

Abstract: Solubility enhancement of poorly aqueous-soluble drugs, like Terbinafine (TBN), is a critical challenge in formulating effective dosage forms. This study focused on developing β-cyclodextrin (β-CD) and polyacrylamide (PAM)-based microgels to address the solubility issue of TBN, classified as a biopharmaceutics classification system class II drug. The microgels were crafted through free radical polymerization, employing methylene bisacylamide as a cross-linker and methacrylic acid as a monomer, initiated by ammonium persulfate. Comprehensive characterizations, including Fourier transform infrared, thermo-gravimetric analysis, differential scanning calorimetry, scanning electron microscopy, powder X-ray diffractometry analysis, Zeta size, and Zeta potential, were conducted. *In vitro* studies, such as drug release and swelling, were performed at pH 1.2. Toxicity analysis in rabbits revealed zero toxicity. These β-CD/PAM microgels successfully enhanced the solubility of TBN.

Keywords: Terbinafine, microgel, β-cyclodextrin, free radical polymerization, polyacrylamide, toxicity

1 Introduction

The emergence of carrier systems to recover target site drug delivery has received a lot of attention among scientists in the field of drug delivery, specifically oral drug delivery systems [1]. Oral ingestion is the most convenient and optimal way of drug delivery owing to its ease of administration, patient safety and compliance, cost effectiveness, and flexibility in the dosage configuration. The pharmacological impact of every orally taken medicament is determined by a complex system of transit from the site of the entrance to the targeted site. The poorly aqueous-soluble drugs having retarded drug absorption due to limited dissolution lead toward insufficient and capricious bioavailability along with gastrointestinal toxicity. For such substances, the gastrointestinal absorption rate is regulated by dissolution. Therefore, numerous approaches such as surfactants, polymeric conjugates, solid dispersions, micronization, complexation, hydrotrophy, and water-soluble carriers have been utilized to enhance drug solubility and dissolution [2].

Novel drug delivery techniques include the development of microgels and nanogels that seem to be the most widely used approaches for the transfer of hydrophilic drugs due to having superior clinical applications such as the water-swollen setup, improved mechanical properties, chemical stability, and physico-chemical adjustability to overcome many of the drawbacks of traditional hydrophobic drug

*** Corresponding author: Kashif Barkat,** Faculty of Pharmacy, The University of Lahore, Lahore, 54000, Punjab, Pakistan; Faculty of Health Sciences, Equator University of Science and Technology, Masaka, Uganda, e-mail: dr.kashif2009@gmail.com
*** Corresponding author: Musaab Dauelbait,** Department of Scientific Translation, Faculty of Translation, University of Bahri, Khartoum, 11111, Sudan, e-mail: musaabelnaim@gmail.com
Saira Akhtar, Nariman Shahid, Maryam Shabbir: Faculty of Pharmacy, The University of Lahore, Lahore, 54000, Punjab, Pakistan
Irfan Anjum: Department of Basic Medical Sciences, Shifa College of Pharmaceutical Sciences, Shifa Tameer-e-Millat University, Islamabad, Pakistan, e-mail: anjuum95@yahoo.com, irfan.scps@stmu.edu.pk
Syed Faisal Badshah: Faculty of Medical and Health Sciences, Department of Pharmacy, University of Poonch, Rawalakot, Azad Jammu and Kashmir, Pakistan, e-mail: faisal.badshah@upr.edu.pk
Samir Ibenmoussa: Laboratory of Therapeutic and Organic Chemistry, Faculty of Pharmacy, University of Montpellier, Montpellier, 34000, France
Yousef A. Bin Jardan: Department of Pharmaceutics, College of Pharmacy, King Saud University, P.O. Box 11451, Riyadh, Saudi Arabia
Mohammed Bourhia: Laboratory of Biotechnology and Natural Resources Valorization, Faculty of Sciences, Ibn Zohr University, 80060, Agadir, Morocco
Ahmad Mohammad Salamatullah: Department of Food Science & Nutrition, College of Food and Agricultural Sciences, King Saud University, 11 P.O. Box 2460, Riyadh, 11451, Saudi Arabia

carriers. Microgels are supramolecular structures that swell when immersed in a solvent. They possess notable features that differ from conventional colloids, dynamic macromolecules, hydrogels, micelles, and vesicles. Likewise, they are much smaller than hydrogels, having dimensions of about 10 nm to 100 μm. Moreover, microgels are adequately soft and small to imitate and cross biological barriers and membranes and can be modified chemically so that they can confer to bio-interfaces and interact with biomolecules. Microgels that can load and then distribute hydrophobic medicines can be developed by creating segmented microgels (e.g., core–shell structures) [3]. By incorporating drugs in such systems, numerous diseases can be treated, e.g., cancer, fungal infections, hypertension, diabetes, etc. Fungal infections are tremendously widespread, such as athlete's foot, fungal nail infection, ringworm, jock itch (an infection in the groin area), and pityriasis versicolor. Although antifungal medicines are efficient in controlling such fungal infections, Terbinafine (TBN) is an effective allylamine antifungal drug that preferentially targets fungal squalene epoxidase. It displays extensive action against molds, yeast, fungus, and dermatophytes. Therefore, TBN is prescribed as a therapy for both oral and topical mycoses. The oral dose of TBN usually includes 250 or 500 mg on a daily basis. It is rather less soluble in aqueous medium and is extremely lipophilic [4].

Polyacrylamide (PAM) is an eminent water-soluble, non-toxic, and biocompatible cross-linked polymer comprised of repeating units of acrylamide monomer [5]. It is utilized in water purification, wound dressing, ophthalmic operations, etc. PAM can be used mutually with artificial and natural polymers for the synthesis of microgels. Furthermore, it possesses the ability to retain a large amount of water due to the presence of hydrophilic groups [6]. Seven glucose units link to form a macrocycle named β-cyclodextrin (β-CD) that produces host–guest interactions with hundreds of chemical agents. Cyclodextrin polymer is a long-chain molecule that functions as an outstanding drug carrier to improve drug dissolution and oral absorption while also ameliorating therapeutic effectiveness [7]. Moreover, methacrylic acid (MAA) was employed as a monomer that dissolves in hot water and is miscible with most organic solvents.

The current research aimed to establish a novel approach to integrate a drug carrier system, i.e., microgel, to resolve the crucial issue by enhancing the solubility of an antifungal drug, TBN. Improved solubility ultimately augments a drug's bioavailability and its therapeutic efficacy. In this work, various ratios of PAM, β-CD, and MAA were employed to synthesize microgel carriers through a cross-linker, methylene bis acrylamide (MBA) by a free radical polymerization technique. This microgel drug delivery system displays pH-responsive behavior. The formulated dosage form was loaded with TBN to release the drug in a manner that can boost patient compliance as well. Henceforth, the solubility and efficacy of the drug can be efficiently improved.

2 Experimental section

2.1 Materials

TBN HCl was a kind gift from Saffron Pharmaceuticals, Faisalabad. β-CD, PAM, MAA, MBA, and ammonium persulphate (APS) were purchased from Sigma Aldrich, UK. Sodium hydroxide (NaOH), potassium chloride (KCl), potassium dihydrogen phosphate (KH_2PO_4), and HCl were purchased from Merck, Germany. All the chemicals utilized were of analytical grade.

2.2 Fabrication of β-CD/PAM microgel system

Seven formulations of β-CD/PAM-based microgel systems were fabricated by changing the quantity of β-CD, MAA, and MBA (Table 1). To synthesize microgels, the most common method, free radical polymerization, was adopted. Accurately weighed quantities of β-CD and PAM were taken to prepare a solution in distilled water separately. Temperature was maintained during the reaction processing until the point where a transparent solution was attained. These solutions were then mixed homogeneously by using a magnetic stirrer. Separate solutions of an initiator, APS, in water and a cross-linker such as MBA in ethanol and distilled water were prepared, which were then incorporated into the reaction mixture dropwise. Then finally, the whole

Table 1: Composition of a β-CD/PAM-based microgel system

Sr. no.	Formulation code	β-CD wt (g)	PAM wt (g)	MAA wt (g)	APS wt (g)	MBA wt (g)
1.	β-CD/PAM 1	0.05	0.03	4	0.1	3
2.	β-CD/PAM 2	0.1	0.03	4	0.1	3
3.	β-CD/PAM 3	0.15	0.03	4	0.1	3
4.	β-CD/PAM 4	0.1	0.03	5	0.1	3
5.	β-CD/PAM 5	0.1	0.03	6	0.1	3
6.	β-CD/PAM 6	0.1	0.03	4	0.1	4
7.	β-CD/PAM 7	0.1	0.03	4	0.1	5

mixture was mixed for 20 min by magnetic stirring and sonicated for 10 min. The final transparent solution was kept in the flask and condensed for 2–3 h at 65°C by using the reflex condensation method. Afterward, the resultant condensed mixture, i.e., white fluffy gel, was poured out of the flask and passed through sieve no. 70, 100, and 200. The attained powder was then dried in an oven at 40°C for 24 h [8,9].

2.3 Drug loading

TBN was loaded into the prepared microgels by the post-loading method. About 250 mg of TBN was dissolved in 6 mL of ethanol at room temperature until the formation of a clear solution. About 1 g of the prepared microgels were mixed separately into 100 mL of pH 1.2 buffer solution with the help of a magnetic stirrer. Then, the entire drug solution was added into the microgel solution slowly and stirred continuouslyfor about 24 h. Continuous stirring was done to ensure uniform mixing of the drug solution and prepared microgel solution. Following the filtration of the ethanol solution having microgels, about 100 mL of distilled water was introduced to rinse the offloaded drug. Finally, these TBN-loaded microgels were dried at 60°C by using a hot-air oven [10].

2.4 Zeta size and zeta potential

The size of TBN-loaded microgels was scrutinized by dynamic light scattering with Zetasizer NanoZS equipment (Malvern, UK) to evaluate whether the size of prepared microgels was within the micrometer range or not. Similarly, the Zeta potential was measured with a Zetasizer NanoZS equipment equipped with a He–Ne laser light source. Zeta potential determination is a significant characterization technique for microgels to estimate the net surface charge [11].

2.5 Morphology of prepared microgels

The structure and composition of microgels were investigated by using a scanning electron microscope (SEM) (JSM-7610F, JEOL). It provides a graphic representation of the surface features of a sample and its composition. Standardized graded alcohol was used to dry the microgels that were coated with gold for approximately 3 min to reduce them to almost 20–30 nm. Finally, samples were scanned, and photomicrographs were recorded and investigated [12].

2.6 Fourier transform infrared spectroscopy (FTIR) studies

FTIR studies were performed to illustrate the presence of functional groups in the formulated microgels [13]. The structural arrangements and spectra of pure drug, loaded, and unloaded microgels were examined using FTIR (Bruker, Germany). By using attenuated total reflectance, the samples were pulverized into acceptable particle sizes and powder was scanned ranging from 4,000 to 500 cm^{-1} [14,15].

2.7 Powder X-ray diffractometry analysis (PXRD)

PXRD is a valuable tool for evaluating CD complex formation in finely ground and crystalline phases. If a real inclusion complex has been generated, the complex's diffraction pattern should be clearly distinguishable from the superposition of each component's diffraction pattern. PXRD study was executed at room temperature by using a diffractometer (Bruker Karlsruhe, Germany). A copper-Kα radiation source was adjusted at a wavelength of 1.542 Å, and pure drug, polymer, and formulated microgels were investigated at an angle of 2θ (10–80°) at a rate of 1° per min [16].

2.8 Thermo-gravimetric analysis (TGA) and differential scanning calorimetry (DSC)

The TGA (TA instrument Q5000 series, West Sussex, UK) was steered out in a simulated environment (78% N, 22% O) at a heating rate of 20°C per minute and a highest temperature of 900°C [17]. DSC is a method used to determine the movement of heat into and out of a subject as a consequence of heat or time when the sample is held at a specific temperature. The transition temperature of glass, melting, crystallization, specific heat capacity, cure procedure, clarity, oxidation behavior, and heat resistance are just a few of the material parameters that may be estimated using this method. For DSC, TA instrument Q2000 series, West Sussex, UK, was used for thermal analysis. For TGA analysis, about 0.5–5 mg sample was placed in an open platinum pan (100 μL) attached to microbalance and heated under dry nitrogen gas from 20 to 600°C, with heat range adjusted at 20°C/min [18].

2.9 Estimation of drug loading

To estimate the percent drug loading, TBN-loaded microgels (100 mg) were repetitively extracted by dipping them

in ethanol until complete extraction of TBN was accomplished. The drug concentration was analyzed spectrophotometrically at 242 nm by using a UV–Vis spectrophotometer (Shimadzu, Japan), and the drug content was calculated by constructing the calibration curve. The total drug concentration of the loaded drug was achieved by summing up all individual drug concentrations. The drug loading (%) of various formulations was determined utilizing below-mentioned equation [19]:

$$\text{Drug loading (\%)} = \frac{\text{Total amount of loaded drug}}{\text{Weight of microgels}} \times 100. \quad (1)$$

2.10 Swelling study

To determine the swelling behavior of formulated microgels, the cellophane membrane was placed in a pH 1.2 buffer solution. A portion of about 100 mg of weighed microgels was loaded in the cellophane membrane separately and then dipped in the solution having pH 1.2. The cellophane membrane was removed after regular time durations. Afterward, the cellophane membrane was hanged until there were no droplets flowing from the membrane, and the weight of swelled particles was examined before the membrane was immersed in the solution once more [20]. The swelling index, Q_t, at time t was calculated using the following expression:

$$Q_t = \frac{m_t - m_o}{m_o}, \quad (2)$$

where m_o is said to be the initial weight of dehydrated microgel taken as weight at zero time, and m_t is the weight after a specific time, t [21]. Swelling behavior was studied in a similar way for various microgel formulations containing varying ratios of β-CD, PAM, and MBA.

2.11 Solubility study

A solubility study was carried out to determine the solubility of TBN hydrochloride microgels in aqueous medium. This was accomplished by dissolving an excess quantity of TBN and TBN-loaded β-CD/PAM microgel complexes in different flasks containing 100 mL distilled water. The flasks were thoroughly shaken on an orbital shaker for 24 h. Afterwards, the suspensions were filtered, diluted accordingly with distilled water, and absorbance was measured by a UV spectrophotometer at 242 nm [19].

2.12 *In vitro* drug release evaluation

The USP dissolution apparatus II was employed to execute the release studies of a TBN-loaded polymeric microgel network. About 125 mg of TBN microgels were incorporated in an empty hard gelatin capsule shell of appropriate size. The capsules were placed in a pH medium of 1.2, imitating the gastric fluid for the dissolution, maintained at 37 ± 1°C for 4 h at 50 rpm. About 5 mL of aliquot samples were withdrawn from the dissolution medium at predetermined time intervals of 0.16, 0.33, 0.5, 0.67, 0.83, 1, 1.5, 2, 2.5, 3, 3.5, and 4 h. The dissolution medium was replaced each time with 5 mL of the same buffer solution to reserve the volume of the dissolution medium. The withdrawn samples were then ultra-centrifuged at 12,000 rpm by using a centrifuge for 10 min. The absorbance of samples was measured by a UV spectrophotometer at a relative wavelength of 242 nm. The amount of drug released at altered time intervals was computed by the calibration curves. Six dilutions (5, 10, 15, 20, 25, 30 µg/mL) were prepared, and the absorbance was measured at 242 nm for the construction of the calibration curve of TBN [22].

2.13 Release kinetics of TBN-loaded microgels

Multiple kinetic models were employed to describe the general pattern of drug release from microgel formulations by using dissolution data.

The following equation was used for the illustration of zero-order release that slowly releases the drug independent of drug concentration in microgel formulation:

$$Q_t = Q_o + Q_{ot} \quad (3)$$

where Q is the amount of drug that is dissolved in a short period of time t, while K is the constant that indicates zero order release [23].

$$\log C = \log C_o - \frac{Kt}{2.303}, \quad (4)$$

where C_o is equal to the initial drug concentration and K is the first-order constant [22,23].

In the literature, a number of predictive concepts for the extraction of water-soluble and poorly water-soluble drugs embedded in semi-solid and solid matrices were devised. Therefore, the model expression is given by the equation:

$$ft = Q = A\sqrt{D(2C - C_s)C_s t}, \quad (5)$$

where Q is the extent of drug released in time (t) per unit area (A), C is the initial concentration of drug, C_s is the solubility of the drug in the matrix media, and D is the diffusivity of the drug molecules (diffusion coefficient) in the matrix substance. The simplified Higuchi model expression is given below:

$$ft = K_H t^{1/2}, \quad (6)$$

where K_H is the Higuchi dissolution constant [24].

In vitro release study data of the microgels was also fitted in the Korsmeyer–Peppas equation, which is as follows:

$$\frac{M_t}{M_\infty} = K \times t^n, \quad (7)$$

where M_t/M_∞ represents the fraction of permeated drug, t is the time, K is the transport constant, and n is the transport exponent [25].

2.14 Oral acute toxicity evaluation

Biocompatibility and toxicological studies of formulated microgels were carried out in accordance with the guidelines of the Organization of Economic Co-operation and Development (OECD). The animal study was approved by the Research and Ethics Committee of The University of Lahore. Six healthy rabbits were taken from the animal house of the Faculty of Pharmacy, The University of Lahore, which follows the recommendations of the guidelines for the care and use of laboratory animals. Rabbits were randomly distributed into two groups (control group and test group) containing three animals each. Test group (B) of rabbits was given 5,000 mg/kg of β-CD/PAM-based microgels on their sixth day, while control group (A) was not given any dose. Subsequently, rabbits of each group were observed for 14 days, where diverse parameters were monitored. At 1st, 7th, and 14th day, rabbits were examined for different parameters such as body weight, signs of sickness, signs of toxicity, skin irritation, allergy, etc. Furthermore, the impact of oral administration of microgel on food and water intake and any kind of behavioral alterations in both control group (A) and treated group (B) were evaluated.

For the blood and hematology study, 5 mL blood sample was taken in EDTA tubes from the marginal vein of rabbits of both groups on the 14th day. Biochemical analysis, including complete blood count (CBC), lipid profile (cholesterol, triglycerides, LDL, HDL), liver function tests (LFTs), and renal function tests (RFTs), was carried out to analyze any kind of deviations.

Subsequently, rabbits were euthanized prior to histological analysis. Notably, vital organs such as heart, kidney, liver, spleen, intestine, and stomach of both control (A) and treated group (B) were separated, and their weight was determined. All the organs were kept in 10% formalin solution in separate jars. Then, the histopathological examination of such organs was performed to appraise any signs of toxicity [14,26].

3 Results and discussion

3.1 Physical analysis

Numerous formulations of β-CD/PAM-based microgels were synthesized by varying the ratios of polymer, cross-linker, and monomer. Microgels were found to be white in appearance. First, after the condensation process, solid but non-uniform microgels were produced. However, after passing through sieve no. 70, 100, 120, and 200, fine and uniform-sized powdered microgels were attained. Finally, after sieving, these microgels were dried in an oven at 45°C for 2–5 h, as shown in Figure 1a.

3.2 Zeta size and Zeta potential

Particle size analysis of the optimized formulation of β-CD/PAM microgels was performed to evaluate the size of the particles to be in the micrometer range. Figure 1b reveals the size range of the β-CD/PAM microgels, which demonstrated that microgel formulation lied in the range of microparticles, i.e., from 1 to 1,000 µm. Moreover, Zeta potential determination is a substantial characterization technique of nanocrystals to estimate the surface charge. The microgels were slightly charged as they displayed a positive Zeta potential of about 18 mV. Hence, it revealed that the developed formulation was stable and uniform.

Attia et al. determined the average particle size of the formulation at ambient temperature by a dynamic laser light scattering apparatus. They also analyzed the zeta potential that indicated that the developed formulations were stable and uniformly dispersed providing analogue findings [27].

3.3 SEM

To evaluate the surface morphology of β-CD/PAM-based microgel blends, SEM was employed. Microgels were

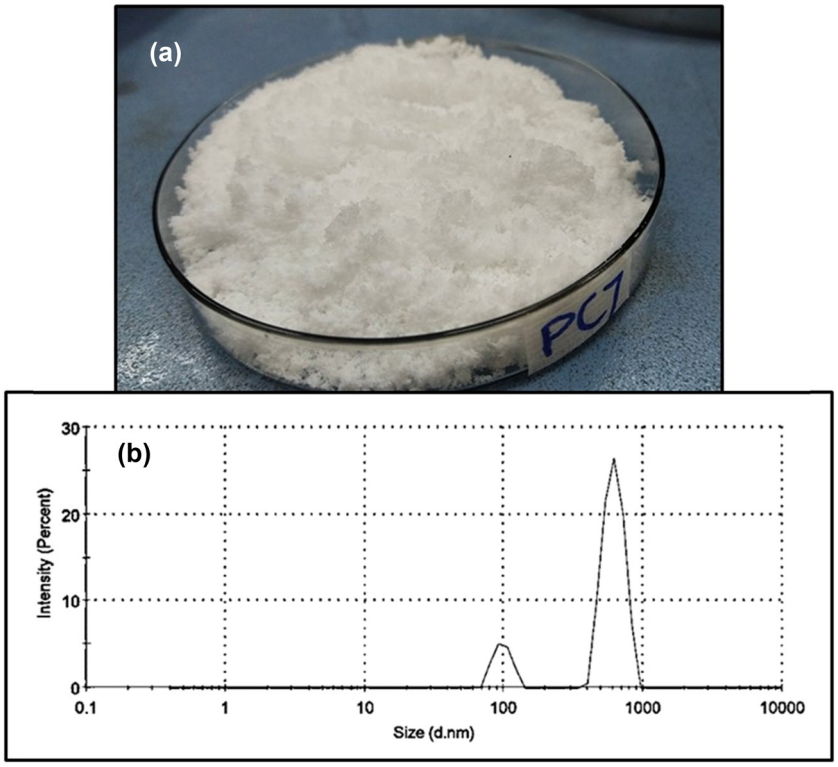

Figure 1: Uniform-sized β-CD/PAM microgels obtained after drying (a) and size distribution by the intensity of optimized microgel formulation (b).

processed at various magnifications to obtain the images. Figure 2a and b shows the SEM micrographs of unloaded microgels. It shows the three-dimensional microgels of β-CD/PAM. A rough and porous structure was observed in the SEM images with well-perceived ridges, which can facilitate significant interaction of solvent with the structure [28]. The SEM micrograph displayed numerous small pores for water absorption. Figure 2c and d represents the SEM micrographs of drug-loaded microgels. The drug can be seen as whitish spots in the SEM images. It displayed that the drug is distributed throughout the microgel system, where the drug particles are embedded in the porous structure of the microgel matrix [29]. Formulated microgels were lyophilized for the removal of the remaining entrapped

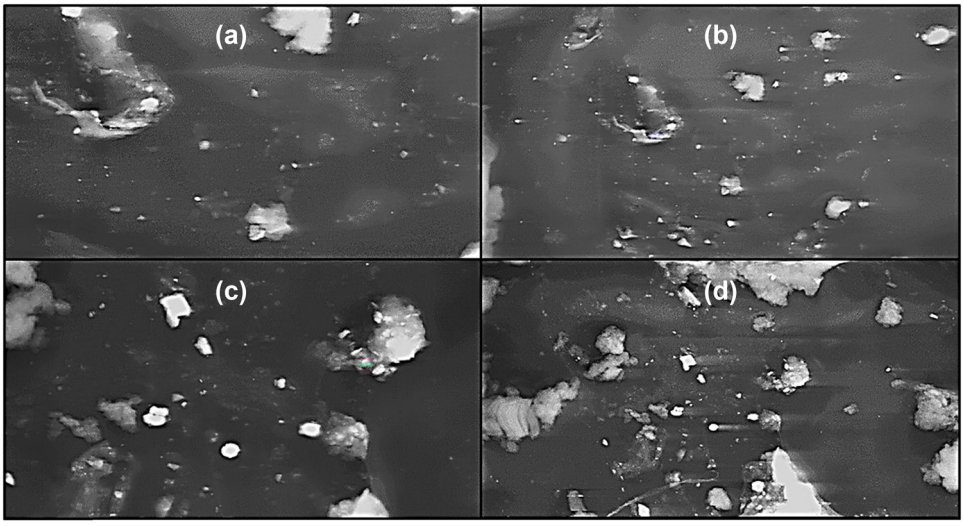

Figure 2: SEM images of (a) and (b) unloaded β-CD/PAM microgels and (c) and (d) loaded β-CD/PAM microgels.

solvent. The porosity of the system was increased due to lyophilization and some structural changes were also observed in the uniformity of the microgels. It was also reported in a previous study that lyophilization increases porosity and brings some changes in structural uniformity. Moreover, porous structure has been observed as a feasible arrangement for enhancing the solubility of poorly aqueous soluble drugs [30]. Likewise, another latest study related to the fabrication and evaluation of maltodextrin microgel revealed comparable SEM results displaying the spherical shape of developed microgels having a magnitude of a few micrometers [31].

3.4 FTIR

The FTIR spectrum of β-CD, PAM, TBN, unloaded β-CD/PAM microgels, and TBN-loaded β-CD/PAM microgels was executed and examined under a wavelength range of 400 to 6,000 cm^{-1}. Results of the FTIR are presented in Figure 3a showing the chemical and structural correlation of microgels.

The FTIR spectrum of β-CD is shown in Figure 3a(a) that demonstrates the peak of β-CD with a slight decrease in the peak intensity. However, the peak of the OH group of β-CD at 3,398 cm^{-1} shifted toward a lower frequency of 3,303 cm^{-1}. The peak at 1,649 cm^{-1} in IR spectra of β-CD was due to water crystallization. Aleem et al. also observed the FTIR pattern of β-CD and found similar findings, as it displayed prominent peaks at 3,390 and 1,647 cm^{-1} (H_2O bending) [32].

The FTIR pattern of PAM in Figure 3a(b) exhibited NH stretching by forming strong bands at 3,166 and 3,281 cm^{-1}, while a peak at 1,538 and 1,645 cm^{-1} demonstrated C═O stretching of acrylamide and NH bending, respectively, demonstrating the vibration modes of the primary amide group. A CH stretching band at 2,915 cm^{-1} was also detected. Freddi et al. also observed PAM that showed strong absorption bands at 3,300 cm^{-1} (NH stretching), 1,660 cm^{-1} (C═O), demonstrating comparable findings [33].

Moreover, the FTIR spectrum of TBN in Figure 3a(c) exhibited a band at 2,345 cm^{-1} indicating C ≡ C stretching, a band at 2,964 cm^{-1} indicating N–H stretching, while the bands at 1,411 and at 1,261 cm^{-1} indicated C═O stretching. Bargir et al. also signposted the FTIR spectrum of TBN and established similar results with major peaks at 2,116 cm^{-1} (C ≡ C stretching), 3,266 cm^{-1} (N–H stretching), and 1,637 cm^{-1} (C═O stretching) [34].

Likewise, the FTIR pattern of unloaded β-CD/PAM microgels is shown in Figure 3a(d). The peaks observed between 1,500 and 2,500 cm^{-1} were mainly due to the presence of OH groups, while the stretching bands at 1,855 to

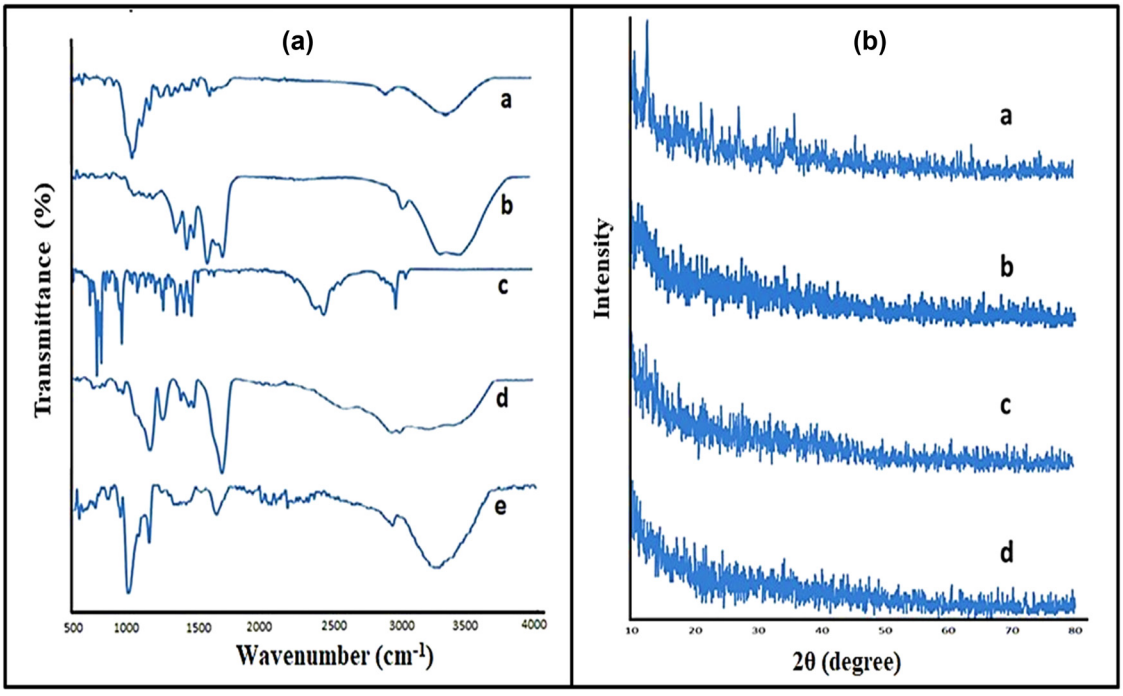

Figure 3: (a) FTIR pattern of ((a) β-CD, (b) PAM, (c) TBN, (d) unloaded, and (e) TBN-loaded β-CD/PAM microgels); (b) XRD pattern of ((a) β-CD, (b) PAM, (c) unloaded, and (d) loaded β-CD/PAM-based microgels).

2,376 cm^{-1} were due to stretching vibration of the CH group of PAMs. Similarly, the FTIR pattern of TBN-loaded β-CD/PAM microgels has been displayed in Figure 3a(e) displaying the existence of various substantial peaks. Such peaks indicated the formation of the polymeric microgel blend via polymerization reaction, while sharp peaks demonstrated the cross-linking of the polymeric microgel blend. Hence, it can be confirmed that the TBN remained stable in the β-CD/PAM microgel system. Similarly, another study demonstrated the analogous results of FTIR confirming the development of theophylline-loaded microgels by the chemical cross-linking of alginate and itaconic acid where itaconic acid interacted with alginate during polymerization reaction and established overlapping of itaconic acid on alginate backbone [35].

3.5 PXRD analysis

PXRD was implemented to determine the amorphous or crystalline nature of β-CD/PAM-based microgels.

The XRD pattern of β-CD displayed sharp and intense peaks, as displayed in Figure 3b. A sharp peak was observed in the 2θ range of 10–15°, as shown in Figure 3b(a). It represented the clear and crystalline nature of the β-CD. Abarca et al. also performed an XRD analysis. They reported that XRD is a useful method for the detection of cyclodextrin in powder or microcrystalline form. Moreover, the XRD pattern of β-CD demonstrated a clear crystalline nature due to its intense and sharp peaks. Furthermore, this pattern accorded with the cage-like structure of the β-CD molecular organization analogous to the currently observed pattern [36].

Likewise, the XRD pattern of PAM displayed some intense peaks formed at 2θ between 10 and 42°, as shown in Figure 3b(b). Such intense peaks specify the slight crystallinity of PAM. Although the overall pattern of the PAM depicts the amorphous nature because of the presence of some intense peaks, some crystallinity can also be observed. Biswal and Singh performed the PXRD analysis of PAM, and the pattern displayed comparable results. The crystalline nature of the polymer, PAM, was also demonstrated [37].

Similarly, the XRD pattern of the loaded β-CD/PAM-based microgel is shown in Figure 3b(c). Here, the XRD pattern exhibited sharp peaks starting at 2θ of about 10°. A slight decline in peak intensity was observed, demonstrating a slight reduction in crystallinity. In contrast, Figure 3b(d) depicted the XRD pattern of the unloaded β-CD/PAM-based microgel. The XRD pattern of unloaded β-CD/PAM-based microgel also demonstrated sharp peaks at the angle 2θ of 10°, indicating that both the loaded and the unloaded formulations were crystalline in nature. As β-CD and PAM are crystalline in nature, the consequential combination of β-CD/PAM microgels also exhibited crystallinity. Su et al. formulated β-CD and acrylamide-based flocculant in which they revealed the synthesis of porous network structure that may cause a huge alteration in the crystalline state, where the AM-β-CD flocculant showed a crystallization peak at around 2θ between 10 and 30° [38].

3.6 TGA and DSC

TGA and DSC of β-CD, PAM, loaded and unloaded formulations were executed as shown in Figure 4a and b, respectively. TGA and DSC of β-CD are shown in Figure 4. In the TGA graph of β-CD, two stages of weight loss were observed. β-CD has shown weight loss, and the first stage began from 90 to 350°C. The second stage displayed weight loss from 250 to 400°C. Aroon et al. have also performed the TGA of the pure β-CD in powder form and concluded a similar graph [39]. The DSC thermogram of β-CD disclosed the first endothermic peak in the range of 64–150°C, while the second peak was observed between 300 and 350°C indicating its melting point [40].

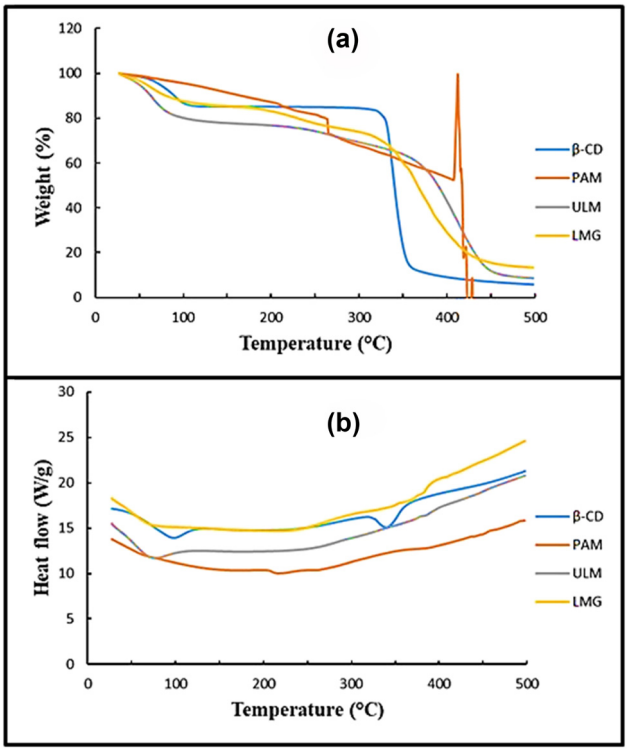

Figure 4: TGA (a) and DSC (b) pattern of β-CD, PAM, unloaded (ULM), and loaded β-CD/PAM microgels (LMG).

TGA of PAM is displayed in Figure 4a. The TGA graph demonstrated that PAM started to decompose at a temperature of 260.12°C and completely decomposed at 410°C. In the DSC graph, PAM responses were found due to the heating of the polymer because of endothermic and exothermic reactions. In the DSC thermogram, an endothermic peak was observed in the range of 175–225°C, indicating the melting point of PAM. Ferreira et al. also observed a thermogram of PAM that showed a T_g value, i.e., 101.4°C, and a T_m value, i.e., 179.9°C. Such results indicated that our formulation exhibited superlative results [41].

Moreover, TGA of β-CD/PAM-based unloaded microgels is shown in Figure 4a. TGA of unloaded formulation depicted the weight loss in three steps: first weight loss occurred at 80°C, second weight loss occurred at 361°C, and finally dropped at 450°C. About 23% weight loss was observed at 198°C and 38% at 361°C. In DSC of the unloaded formulation, an endothermic peak was observed in the range of 40–125°C.

Similarly, TGA of β-CD/PAM-based loaded microgels depicted the weight loss that occurred in three steps with the escalation in temperature: first weight loss occurred at 56°C, second weight loss occurred at 300°C, and finally dropped to 410°C. A 5% weight loss was observed at about 56°C, while 26% weight loss was observed at 300°C, displaying the stability of drug-loaded microgels. In DSC of loaded formulation, endothermic peaks were observed in the range of 50°C–230°C, and finally, a diminished peak was observed between 350 and 420°C. Sorkhabi et al. prepared and characterized novel microgels loaded with SiO_2 nanoparticles and demonstrated similar results where the residual weight percent displayed by core–shell microgel was about 31.6%. Concisely, the findings depicted that the presence of silica nanoparticles leads to improvement in the thermal stability of microgel preparations as compared to the raw copolymer [29].

3.7 Quantification of drug loading into microgels

Drug loading was accomplished by post-loading technique by incorporating TBN solution in microgel solution under constant stirring as described previously. Swelling plays a crucial role in drug loading. The greater amount of drug can be loaded by the system that displays ample swelling due to the larger pore size that allows penetration of drug molecules into the pores of the microgel network. Estimation of drug loading was carried out on all microgel formulations, as displayed in Figure 5. The % drug loading was observed to

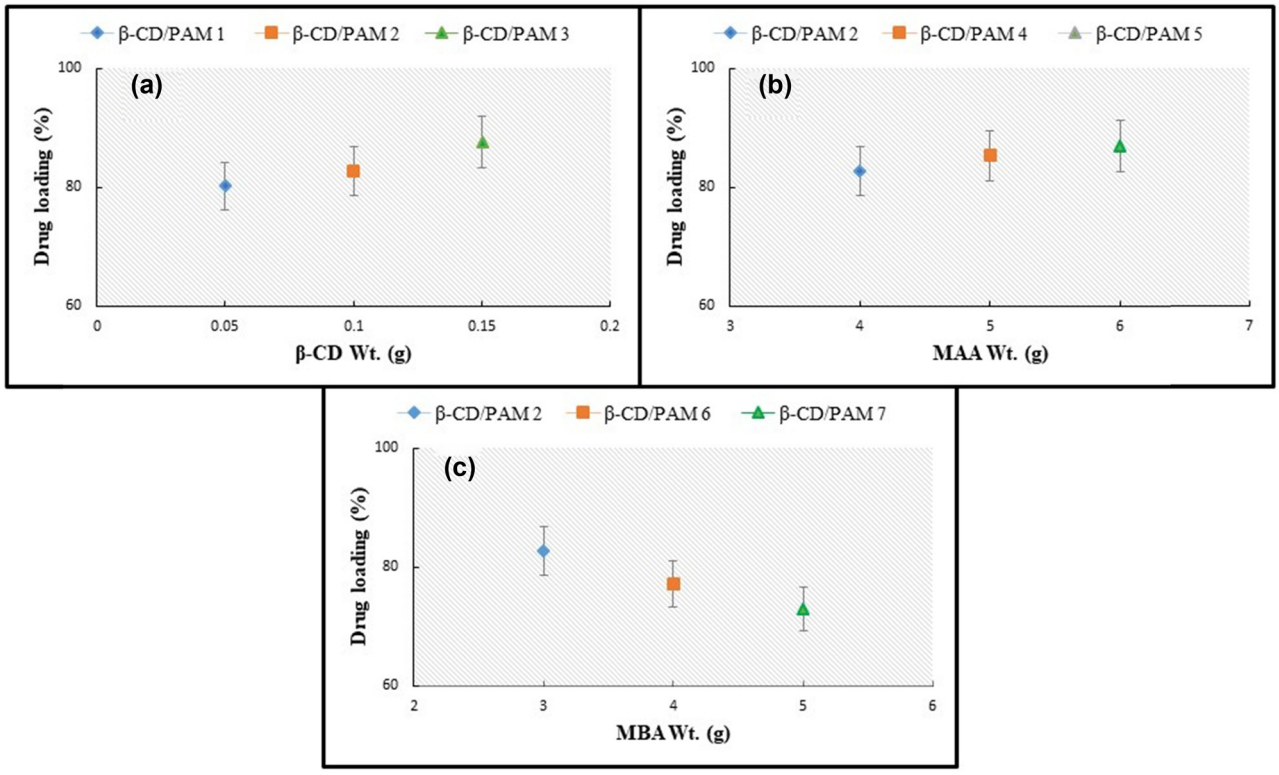

Figure 5: Drug loading of β-CD/PAM-based microgels at varying concentrations of β-CD (a), MAA (b), and MBA (c).

be enhanced with increasing concentrations of β-CD and PAM as the swelling was also boosted by increasing the concentration of β-CD and MAA. Contrary to β-CD and MAA, the % drug loading was observed to be reduced as the concentration of MBA increased. This happened probably due to an increase in bulk density that resulted in dwindled water penetration and ultimately reduced swelling as well as drug loading capacity. Moreover, the formulations coded as β-CD/PAM 3 and β-CD/PAM 5 displayed maximum drug loading of 87.3 and 86.9%, respectively. Suhail et al. synthesized aspartic acid-loaded microgels and displayed similar findings about drug loading where % drug loading increased by increasing the monomer (AMPS) and aspartic acid concentration, while a reduction in % drug loading was observed as the concentration of the cross-linker (MBA) increased [42].

3.8 Swelling study of β-CD/PAM-based microgels

Three β-CD-based microgel formulations were prepared in combination with PAM by the free radical polymerization method. By incorporating different concentrations of β-CD in a β-CD/PAM-based microgel system, the prepared formulations were coded as β-CD/PAM 1, β-CD/PAM 2, and β-CD/PAM 3 containing β-CD equivalent to 0.05, 0.1, and 0.15 g, respectively. Figure 6a displayed that β-CD/PAM 1 exhibited minimum swelling due to less amount of β-CD present in it, while β-CD/PAM 3 exhibited maximum swelling due to greater amount of β-CD present in it. Therefore, it can be concluded that by adding more quantity of β-CD, the swelling response was augmented. Uyanga et al., upon the hydrolytic analysis, reported that the incorporation of β-CD enhanced the degree of cross-linking for hydrogels H1 and H3 and demonstrated that H1 displayed the best microstructure formation [43].

Similarly, the effect of altering the amount of MAA on β-CD/PAM-based microgels was observed. Diverse concentrations of MAA were employed, i.e., 4, 5, and 6 g in the microgels coded as β-CD/PAM 2, β-CD/PAM 4, and β-CD/PAM 5, respectively. Hence, it was observed that with the increase in the MAA ratio, water uptake increases, which resulted in increased swelling behavior of β-CD/PAM-based microgels. Henceforth, β-CD/PAM 5 displayed a greater swelling response due to the supplementary MAA ratio and vice versa in the case of β-CD/PAM2. Bajpai and Singh also concluded that with an increase in the cross-linking ratio, the water uptake at different time intervals improved. This was simply due to the

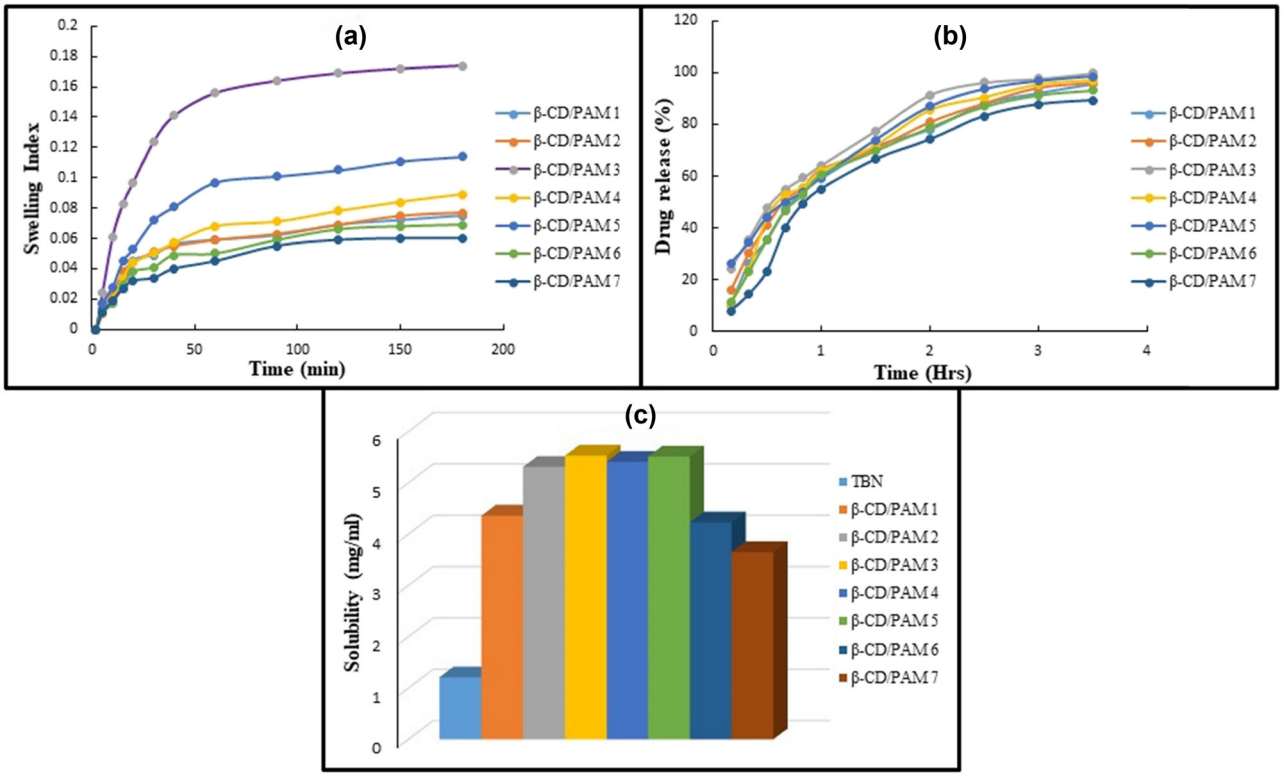

Figure 6: Swelling behavior (a), drug release pattern (b), and solubility study (c) of β-CD/PAM-based microgels at pH 1.2.

fact that with the increase in the cross-linking ratio, an increase in the free space available between cross-links occurs. They concluded with the same results as that of our findings [44].

Moreover, varying amounts of MBA were employed in formulating microgels, i.e., 3, 4, and 5 g in the case of β-CD/PAM 2, β-CD/PAM 6, and β-CD/PAM 7, respectively. By increasing the amount of MBA, swelling decreased, as shown in Figure 6a. This happened because of an increase in cross-linking within the microgels, which led to decreased swelling. It was observed that with an increased ratio of cross-linkers, there was an escalation in the degree to which microgels were tightly bound. Kratz et al. analyzed the swelling behavior for BIS cross-linked particles. It was observed that the swelling capacity decreased with increasing cross-linker concentration similar to our findings [45].

3.9 Solubility study

The solubilities of TBN- and TBN-loaded β-CD/PAM complex were determined in distilled water. It has been reported that the solubility of TBN is highly pH dependent, being higher at acidic pH and significantly lower (1%) at alkaline pH. Moreover, as reported earlier, TBN displays very limited aqueous solubility of about 1.21 mg/mL. When dissolution results of various formulations were compared, it was found that the prepared microgels containing the same concentration of TBN displayed an escalation in absorbance than TBN. The absorbance increased from 0.034 to 0.092 after 2 h in the case of TBN HCl and TBN-loaded microgels, respectively. Hence, it is proved that the goal of our formulation has been achieved to provide enhanced solubility for the purpose of achieving improved therapeutic efficacy. Moreover, β-CD/PAM 3 formulation displayed a 4.56 folds increase in the solubility from 1.21 to 5.53 mg/mL. Hence, solubility of TBN enhanced significantly after being formulated into microgels.

3.10 *In vitro* drug release of TBN

A drug release study of β-CD/PAM microgels loaded with TBN was executed and is presented in Figure 6b. Seven microgel formulations loaded with TBN were placed in the USP dissolution apparatus II at 37°C containing an acidic buffer of pH 1.2. Drug release (% age) was determined with the help of a calibration curve. TBN, being highly lipophilic and basic in nature, exhibits maximum solubility in an acidic medium and vice versa in an alkaline medium. The *in vitro* drug release profile followed the same pattern as observed for the swelling of microgels. Drug release was observed to be enhanced with increasing concentrations of β-CD and MAA. An inverse relationship was observed between cross-linker concentration and release of drug from the microgels, possibly due to increased cross-linking among microgel network, availability of less free spaces for drug liberation, and also lessened volume of dissolution medium that penetrated into the microgels. Hence, β-CD/PAM 7, containing the maximum amount of MBA, displayed a minimum drug release of 89.25%. Whereas β-CD/PAM 3 and β-CD/PAM 5, containing the maximum amount of β-CD and MAA, exhibited maximum drug release of 99.92 and 98.6%, respectively. Hassan et al. fabricated TBN HCL-loaded nanogels for topical drug delivery and displayed comparable findings where, contrary to AA, the drug release (%) declined by increasing the amount of cross-linker (MBA). Formulation AA7 displayed a maximum drug release of about 92% with a minimum MBA concentration of 2% w/v [46].

3.11 Kinetic modeling

Zero-order, first-order, Higuchi, and Korsmeyer–Peppas mathematical models were applied to dissolution data of β-CD/PAM microgels in order to study the release pattern of TBN. All seven formulations ranging from β-CD/PAM 1 to β-CD/PAM 7 were subjected to mathematical models. Here, all the formulations were best fitted to the first order, as evident from the value of regression coefficient (R^2), i.e., 0.9804–0.9970, as represented in Table 2. In addition, all the formulations from β-CD/PAM 1 to β-CD/PAM 7 followed the Korsmeyer–Peppas model as well as its R^2 value ranged from 0.9765 to 0.9931. Moreover, the value of n (diffusion exponent) was observed to be >0.45 and <0.89, indicating

Table 2: Kinetic modeling of TBN loaded microgels

Microgel formulations	Zero-order	First-order	Higuchi	Korsmeyer–Peppas	
	R^2	R^2	R^2	R^2	N
β-CD/PAM 1	0.8741	0.9869	0.9565	0.9831	0.532
β-CD/PAM 2	0.8556	0.9970	0.9604	0.9925	0.614
β-CD/PAM 3	0.8846	0.9910	0.9588	0.9967	0.621
β-CD/PAM 4	0.8501	0.9868	0.9521	0.9830	0.568
β-CD/PAM 5	0.8353	0.9804	0.9360	0.9952	0.642
β-CD/PAM 6	0.8373	0.9887	0.9011	0.9814	0.585
β-CD/PAM 7	0.8728	0.9932	0.9476	0.9777	0.593

Table 3: Clinical outcomes, hematology, biochemical blood evaluation and impact of orally dispensed microgels on organ weight of rabbits

Finding parameters	Group A (control)	Group B (treated with microgel) 5 g/kg
Signs of indisposition	Nil	Nil
Body weight (kg)		
Prior to therapy	1.39 ± 0.04	1.32 ± 0.05
Day 1	1.43 ± 0.03	1.36 ± 0.06
Day 7	1.48 ± 0.05	1.49 ± 0.06
Day 14	1.52 ± 0.03	1.50 ± 0.03
Water utilization (mL)		
Prior to treatment	196.76 ± 1.23	195.66 ± 2.33
Day 1	199.44 ± 1.45	193.56 ± 2.34
Day 7	192.45 ± 2.32	194.76 ± 1.96
Day 14	194.66 ± 1.22	194.58 ± 1.45
Food intake (g)		
Preliminary to treatment	74.33 ± 1.14	73.67 ± 2.33
Day 1	76.77 ± 1.23	74.54 ± 2.78
Day 7	72.65 ± 3.45	78.56 ± 1.56
Day 14	73.55 ± 1.24	77.23 ± 1.34
Sickness	Nil	Nil
Ocular toxicity	Nil	Nil
Skin allergy/irritation	Nil	Nil
Mortality	Nil	Nil
Hematology		
Hb (10–15) g/dL	13.8 ± 0.45	13.4 ± 0.56
RBCs × 10^6/mm^3	5.77 ± 0.04	6.94 ± 0.05
Platelets × 10^3/μL	246 ± 3.45	234 ± 3.85
Lymphocytes (%)	27.8 ± 0.12	29.6 ± 0.16
Neutrophils (%)	69.6 ± 0.22	48.6 ± 0.13
Monocytes (%)	4.6 ± 0.02	5.6 ± 0.03
HCT (%)	41.7 ± 0.12	42.5 ± 0.18
MCV (fL)	66.1 ± 0.25	61.2 ± 0.31
MCH (pg)	21.5 ± 0.33	19.3 ± 0.32
MCHC (g/dL)	32.5 ± 0.43	31.5 ± 0.21
TLC × 10^3/μL	11.15 ± 0.11	10.44 ± 0.32
Biochemical evaluation		
Lipid profile		
Cholesterol (mg/dL)	34 ± 1.12	30 ± 1.31
Triglycerides (mg/dL)	67 ± 0.18	59 ± 0.09
HDL (mg/dL)	17 ± 0.02	18 ± 0.07
LDL (mg/dL)	16 ± 1.32	13 ± 1.44
Liver function tests (LFTs)		
Total bilirubin (mg/dL)	0.1 ± 0.02	0.1 ± 0.02
Alk. phosphate U/L	125 ± 0.19	128 ± 0.12
ALT U/L	64 ± 0.03	61 ± 0.12
AST U/L	48 ± 0.13	44 ± 0.16
RFTs		
Blood urea	40 ± 0.11	39 ± 0.09
S/creatinine	0.7 ± 0.01	0.9 ± 0.02
Organ weight (g) of rabbits		
Heart	3.89 ± 0.03	4.23 ± 0.07
Liver	31.98 ± 2.45	28.91 ± 2.58
Kidney	3.45 ± 0.98	3.6 ± 0.77
Spleen	0.43 ± 0.04	0.38 ± 0.03
Intestine	4.25 ± 0.21	4.11 ± 0.24
Lungs	7.62 ± 0.34	7.99 ± 0.49
Stomach	13.45 ± 0.44	14.55 ± 0.52

that the drug was released from the polymeric microgels by anomalous mechanism of drug transport. Hence, the drug was liberated from the polymeric microgels by non-Fickian diffusion demonstrating a release pattern based on both diffusion and dissolution. As all formulations did not follow the zero-order kinetics, it means that it does not give a constant release of drug independent of drug concentration. Similar findings were displayed by Hassan et al. where the TBN release followed the first-order and Korsmeyer–Peppas model based on R^2 values. The value of release exponent, n, for all formulations, ranged between 0.581 and 0.860, exposing that all formulations presented anomalous release, i.e., based on both swelling and diffusion [46].

3.12 Acute oral toxicity study

A 14-day oral toxicity study on β-CD/PAM microgels was executed on rabbits according to the OECD guidelines. Six healthy rabbits having approximate weights between 1,000 and 1,500 g were selected and randomly disseminated into two groups labeled as Control group (Group A) and Treatment group (Group B). The control group entailing three rabbits was not given any medication, while the medicated group comprised of three rabbits was given 500 mg of microgel capsules each. On the 1st, 7th, and 14th day, rabbits were examined for diverse parameters such as body weight, sickness, skin irritation, food and water utilization, behavior patterns, signs of indisposition, etc., as conferred in Table 3. No signs of sickness, indication of toxicity of eyes or running nose, nor any kind of skin allergy was noticed [47]. The eating pattern of treatment group B was normal, and they also gained weight similar to that of the control group A [48]. Clinical observations justified that there was no paramount transmogrification in body weight and food exhaustion of rabbits along with zero mortality throughout the toxicity study.

Biochemical analysis was carried out to analyze any kind of changes in copious parameters such as CBC, lipid profile, liver function tests (LFTs), and renal function tests (RFTs), as displayed in Table 3. Complete blood count

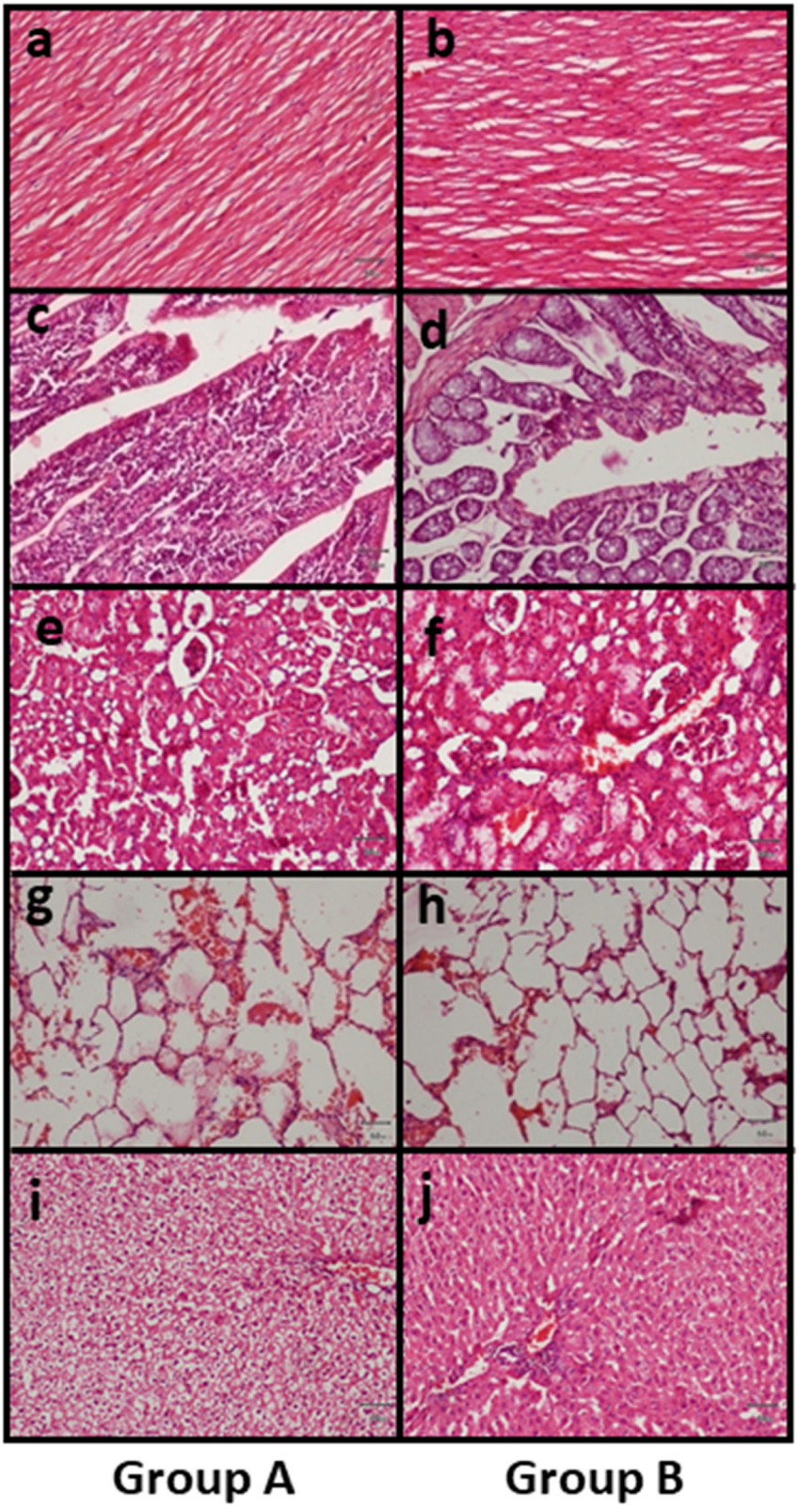

Figure 7: Histological assessment of control (A) and treated group (B) of rabbit's vital organs: Heart (a) and (b), intestine (c) and (d), kidney (e) and (f), lungs (g), and (h) and liver (i) and (j).

parameters of group (B) were in the standard reference range, similar to the control group (A) values, as well as the values of lipid profile, LFT, and RFT indicated that the formulated microgels are likely to be nontoxic. Divergent specifications concerning biochemical atomization were envisaged as convened in Table 3. Biochemical findings of both groups were discerned to be within the normal range. It has been observed that the developed microgels administration did not alter any of such biochemical parameters to toxic levels [49,50].

After withdrawing the blood sample, each rabbit was sacrificed. Vital organs such as heart, intestine, liver, kidney, lungs, stomach, and spleen of both control and treatment groups were separated, and their weight was determined. The weight of all the organs of rabbits of both the groups, i.e., Group A and Group B, was found to be within normal ranges. All the organs were placed separately in 10% formalin solution, and afterward, the histopathological investigation of crucial organs was executed. After microscopic examination of such organs, no significant changes were noticed in either group and, hence, proved that β-CD/PAM microgels were non-toxic because they did not cause any significant changes in the organs of either group of rabbits. No variation in the histopathological investigation of vital organs of treatment group B from the control group A was revealed, as demonstrated in Figure 7. The pericardium, myocardium, and endocardium of treatment group B seemed normal in shape and cardiac muscles did not illustrate any kind of hypertrophy [51]. The mucosal lining of the intestines was free of ulcer symptoms. Moreover, the lungs of the rabbits exhibited no signs of arteriosclerosis nor alveolar or bronchial damage. The size and shape of the kidney were normal. Likewise, liver lobules of treatment group B displayed clear dividing lines, similar to control group A [52]. Henceforth, no substantial difference in histopathological observation, hematological, and biochemical parameters was established, attributing to the normal functioning of vital organs of both control and treatment groups [53]. Additionally, Cheaburu-Yilmaz et al. recently reported extensive information on the toxicity evaluation of oral melatonin nano/microparticles, where a slight hepatotoxicity was detected following drug administration in microparticle formulation to mice, as demonstrated by histopathology and clinical biochemistry of blood [54].

4 Conclusion

It can be concluded that β-CD/PAM-based microgels were successfully formulated through the process of free radical polymerization and reflux condensation technique. PAM and β-CD were employed as polymers, MAA was used as a monomer, while MBA was utilized as a cross-linker. β-CD/PAM-based microgels were subjected to various characterization processes such as FTIR, SEM, TGA, DSC, XRD, swelling studies, Zeta size, and Zeta potential. The results provided evidence that this work astounded some of the common problems associated with the solubility of the poorly aqueous soluble drug, TBN, which in turn can increase the therapeutic efficacy of the drug. By applying kinetic modeling, all seven formulations followed the first order as well as the Korsmeyer–Peppas model based on the value of the regression coefficient. SEM images demonstrated the formation of the desired porous structure. SEM, Zeta size, and Zeta potential indicated the morphology of microgels as well as the specific micron size of the formulation. Moreover, the solubility of the microgels loaded with TBN was found to be enhanced when compared with pure TBN. Moreover, the fabricated microgels exhibited pH-dependent swelling and drug release. Similarly, toxicity studies of β-CD/PAM-based microgels demonstrated the non-toxic as well as biocompatible nature of synthesized microgels. Hence, the solubility enhancement, pH-dependent swelling, and drug release behavior proved that the TBN-loaded microgel formulation could provide a platform for other poorly aqueous-soluble drugs also to enhance their efficacy and solubility as per the need of the future. Furthermore, *in vivo* bioavailability studies can be performed as well on the currently developed TBN loaded microgels in the future to further boost their applicability and efficacy.

Acknowledgments: The authors extend their appreciation to the Researchers Supporting Project number (RSP-2024R437), King Saud University, Riyadh, Saudi Arabia.

Funding information: This work is financially supported by the Researchers Supporting Project number (RSP-2024R437), King Saud University, Riyadh, Saudi Arabia.

Author contributions: Saira Akhtar: conceptualization, methodology, original draft writing. Kashif Barkat: conceptualization. Nariman Shahid: writing (original draft, reviewing, and editing), data. Irfan Anjum: investigation, data curation. Syed Faisal Badshah: methodology, formal analysis. Maryam Shabbir: formal analysis. Samir Ibenmoussa: resources. Yousef A. Bin Jardan: resources. Mohammed Bourhia: resources. Musaab Dauelbait, Ahmad Mohammad Salamatullah: resources, validation, data curation.

Conflict of interest: The authors declared no potential conflicts of interest with respect to the research, authorship, and/or publication of this article.

Ethical approval: The toxicity study conducted on rabbits was approved by the Pharmacy Research Ethics Committee (PREC), University of Lahore, Pakistan (Vide ref. no. IREC-2017.142A).

Data availability statement: Data will be available upon request from the corresponding author.

References

[1] Rajera R, Nagpal K, Singh SK, Mishra DN. Niosomes: a controlled and novel drug delivery system. Biol Pharm Bull. 2011;34(7):945–53.

[2] Klueglich M, Ring A, Scheuerer S, Trommeshauser D, Schuijt C, Liepold B, et al. Ibuprofen extrudate, a novel, rapidly dissolving ibuprofen formulation: relative bioavailability compared to ibuprofen lysinate and regular ibuprofen, and food effect on all formulations. J Clin Pharmacol. 2005;45(9):1055–62.

[3] Dave R, Randhawa G, Kim D, Simpson M, Hoare T. Microgels and nanogels for the delivery of poorly water-soluble drugs. Mol Pharm. 2022;19(6):1704–21

[4] Gaba B, Fazil M, Khan S, Ali A, Baboota S, Ali J. Nanostructured lipid carrier system for topical delivery of terbinafine hydrochloride. Bull Fac PharmCairo Univ. 2015;53(2):147–59.

[5] Yang T-H. Recent applications of polyacrylamide as biomaterials. Recent Pat Mater Sci. 2008;1(1):29–40.

[6] Nardo T, Carmagnola I, Ruini F, Caddeo S, Calzone S, Chiono V, et al. Synthetic biomaterial for regenerative medicine applications. In Kidney transplantation, bioengineering and regeneration. Elsevier; 2017. p. 901–21.

[7] Gidwani B, Vyas A. Synthesis, characterization and application of epichlorohydrin-β-cyclodextrin polymer. Colloids Surf B: Biointerfaces. 2014;114:130–7.

[8] Nishizawa Y, Minato H, Inui T, Uchihashi T, Suzuki D. Nanostructures, thermoresponsiveness, and assembly mechanism of hydrogel microspheres during aqueous free-radical precipitation polymerization. Langmuir. 2020;37(1):151–9.

[9] Durmaz S, Okay O. Acrylamide/2-acrylamido-2-methylpropane sulfonic acid sodium salt-based hydrogels: synthesis and characterization. Polymer. 2000;41(10):3693–704.

[10] Sarfraz RM, Khan MU, Mahmood A, Akram MR, Minhas MU, Qaisar MN, et al. Synthesis of co-polymeric network of carbopol-g-methacrylic acid nanogels drug carrier system for gastro-protective delivery of ketoprofen and its evaluation. Polym Technol Mater. 2020;59(10):1109–23.

[11] Sahiner N, Sagbas S, Yoshida H, Lyon LA. Synthesis and properties of inulin based microgels. Colloids Interface Sci Commun. 2014;2:15–8.

[12] Suhail M, Xie A, Liu J-Y, Hsieh W-C, Lin Y-W, Minhas MU, et al. Synthesis and in vitro evaluation of aspartic acid based microgels for sustained drug delivery. Gels. 2022;8(1):12.

[13] Costa-Júnior ES, Barbosa-Stancioli EF, Mansur AA, Vasconcelos WL, Mansur HS. Preparation and characterization of chitosan/poly (vinyl alcohol) chemically crosslinked blends for biomedical applications. Carbohydr Polym. 2009;76(3):472–81.

[14] Abdullah O, Usman Minhas M, Ahmad M, Ahmad S, Barkat K, Ahmad A. Synthesis, optimization, and evaluation of polyvinyl alcohol-based hydrogels as controlled combinatorial drug delivery system for colon cancer. Adv Polym Technol. 2018;37(8):3348–63.

[15] Barkat K, Ahmad M, Minhas MU, Khalid I. Oxaliplatin-loaded crosslinked polymeric network of chondroitin sulfate-co-poly (methacrylic acid) for colorectal cancer: Its toxicological evaluation. J Appl Polym Sci. 2017;134(38):45312.

[16] Zhao X, Li W, Luo Q, Zhang X. Enhanced bioavailability of orally administered flurbiprofen by combined use of hydroxypropyl-cyclodextrin and poly (alkyl-cyanoacrylate) nanoparticles. Eur J Drug Metab Pharmacokinet. 2014;39(1):61–7.

[17] Senna AM, Novack KM, Botaro VR. Synthesis and characterization of hydrogels from cellulose acetate by esterification crosslinking with EDTA dianhydride. Carbohydr Polym. 2014;114:260–8.

[18] Minhas MU, Ahmad M, Anwar J, Khan S. Synthesis and characterization of biodegradable hydrogels for oral delivery of 5-fluorouracil targeted to colon: screening with preliminary in vivo studies. Adv Polym Technol. 2018;37(1):221–9.

[19] Sarfraz RM, Ahmad M, Mahmood A, Ijaz H. Development, in vitro and in vivo evaluation of pH responsive β-CD-comethacrylic acid-crosslinked polymeric microparticulate system for solubility enhancement of rosuvastatin calcium. Polym Technol Eng. 2018;57(12):1175–87.

[20] Khan KU, Akhtar N, Minhas MU. Poloxamer-407-co-poly (2-acrylamido-2-methylpropane sulfonic acid) cross-linked nanogels for solubility enhancement of olanzapine: synthesis, characterization, and toxicity evaluation. AAPS PharmSciTech. 2020;21(5):1–15.

[21] Khalid I, Ahmad M, Minhas MU, Barkat K. Synthesis and evaluation of chondroitin sulfate based hydrogels of loxoprofen with adjustable properties as controlled release carriers. Carbohydr Polym. 2018;181:1169–79.

[22] Murtaza G, Ahmad M. Microencapsulation of tramadol hydrochloride and physicochemical. J Chem Soc Pak. 2009;31(4):511–9.

[23] Costa P, Sousa Lobo J. Evaluation of mathematical models describing drug release from estradiol transdermal systems. Drug Dev Ind Pharm. 2003;29(1):89–97.

[24] Costa P, Lobo JMS. Modeling and comparison of dissolution profiles. Eur J Pharm Sci. 2001;13(2):123–33.

[25] Wu IY, Bala S, Škalko-Basnet N, Di Cagno MP. Interpreting non-linear drug diffusion data: Utilizing Korsmeyer-Peppas model to study drug release from liposomes. Eur J Pharm Sci. 2019;138:105026.

[26] Barkat K, Ahmad M, Usman Minhas M, Khalid I, Nasir B. Development and characterization of pH-responsive polyethylene glycol-co-poly (methacrylic acid) polymeric network system for colon target delivery of oxaliplatin: Its acute oral toxicity study. Adv Polym Technol. 2018;37(6):1806–22.

[27] Attia A, Enan M, Hashish ET, AAMH, El-kannishy S, Gardouh AR, Tawfik K, M, et al. Chemopreventive effect OF 5-flurouracil polymeric hybrid PLGA-lecithin nanoparticles against colon dysplasia model in mice and impact on p53 Apoptosis. Biomolecules. 2021;11(1):109.

[28] Badshah SF, Minhas MU, Khan KU, Barkat K, Abdullah O, Munir A, et al. Structural and in-vitro characterization of highly swellable β-cyclodextrin polymeric nanogels fabricated by free radical

polymerization for solubility enhancement of rosuvastatin. Part Sci Technol. 2023;41(8):1131–45.
[29] Sorkhabi TS, Samberan MF, Ostrowski KA, Majka TM, Piechaczek M, Zajdel P. Preparation and characterization of novel microgels containing nano-SiO2 and copolymeric hydrogel based on poly (Acrylamide) and poly (Acrylic Acid): morphological, structural and swelling studies. Materials. 2022;15(14):4782.
[30] Badshah SF, Akhtar N, Minhas MU, Khan KU, Khan S, Abdullah O, et al. Porous and highly responsive cross-linked β-cyclodextrin based nanomatrices for improvement in drug dissolution and absorption. Life Sci. 2021;267:118931.
[31] Sahiner M, Gungor B, Silan C, Demirci S, Erdogan H, Ayyala RS, et al. Synthesis and characterization of poly (Maltodextrin) microgel from maltodextrin as drug delivery system. Reactive Funct Polym. 2024;195:105826.
[32] Aleem O, Kuchekar B, Pore Y, Late S. Effect of β-cyclodextrin and hydroxypropyl β-cyclodextrin complexation on physicochemical properties and antimicrobial activity of cefdinir. J Pharm Biomed Anal. 2008;47(3):535–40.
[33] Freddi G, Tsukada M, Beretta S. Structure and physical properties of silk fibroin/polyacrylamide blend films. J Appl Polym Sci. 1999;71(10):1563–71.
[34] Bargir TN, Aj A, Sa P. Composition of terbinafine HCL polymeric gel for mucosal drug delivery. IJBPAS. 2016;5(9):2146–68.
[35] Suhail M, Li X-R, Liu J-Y, Hsieh W-C, Lin Y-W, Wu P-C. Fabrication of alginate based microgels for drug-sustained release: In-vitro and in-vivo evaluation. Int J Biol Macromolecules. 2021;192:958–66.
[36] Abarca RL, Rodriguez FJ, Guarda A, Galotto MJ, Bruna JE. Characterization of beta-cyclodextrin inclusion complexes containing an essential oil component. Food Chem. 2016;196:968–75.
[37] Biswal D, Singh R. Characterisation of carboxymethyl cellulose and polyacrylamide graft copolymer. Carbohydr Polym. 2004;57(4):379–87.
[38] Su Q, Wang Y, Sun W, Liang J, Meng S, Wang Y, et al. Synthesis and characterization of cyclodextrin-based acrylamide polymer flocculant for adsorbing water-soluble dyes in dye wastewater. R Soc open Sci. 2020;7(1):191519.
[39] Aroon M, Ismail A, Matsuura T. Beta-cyclodextrin functionalized MWCNT: A potential nano-membrane material for mixed matrix gas separation membranes development. Sep Purif Technol. 2013;115:39–50.
[40] Raju N, Singh A, Benjakul S. Recovery, reusability and stability studies of beta cyclodextrin used for cholesterol removal from shrimp lipid. RSC Adv. 2021;11(37):23113–21.
[41] Ferreira L, Vidal M, Gil M. Design of a drug-delivery system based on polyacrylamide hydrogels. Evaluation of structural properties. Chem Educator. 2001;6(2):100–3.
[42] Suhail M, Xie A, Liu J-Y, Hsieh W-C, Lin Y-W, Minhas MU, et al. Synthesis and in vitro evaluation of aspartic acid based microgels for sustained drug delivery. Gels. 2021;8(1):12.
[43] Uyanga KA, Okpozo OP, Onyekwere OS, Daoud WA. Citric acid crosslinked natural bi-polymer-based composite hydrogels: Effect of polymer ratio and beta-cyclodextrin on hydrogel microstructure. React Funct Polym. 2020;154:104682.
[44] Bajpai SK, Singh S. Analysis of swelling behavior of poly (methacrylamide-co-methacrylic acid) hydrogels and effect of synthesis conditions on water uptake. React Funct Polym. 2006;66(4):431.
[45] Kratz K, Lapp A, Eimer W, Hellweg T. Volume transition and structure of triethyleneglycol dimethacrylate, ethylenglykol dimethacrylate, and N, N′-methylene bis-acrylamide cross-linked poly (N-isopropyl acrylamide) microgels: a small angle neutron and dynamic light scattering study. Colloids Surf A: Physicochem Eng Asp. 2002;197(1-3):55–67.
[46] Hassan S, Khalid I, Hussain L, Imam MT, Shahid I. Topical delivery of terbinafine HCL using nanogels: a new approach to superficial fungal infection treatment. Gels. 2023;9(11):841.
[47] Sirviö JA, Liimatainen H, Visanko M, Niinimäki J. Optimization of dicarboxylic acid cellulose synthesis: reaction stoichiometry and role of hypochlorite scavengers. Carbohydr Polym. 2014;114:73–7.
[48] Seralini G-E, Clair E, Mesnage R, Gress S, Defarge N, Malatesta M, et al. Long term toxicity of a Roundup herbicide and a Roundup-tolerant genetically modified maize. Food Chem Toxicol. 2012;50:4221.
[49] Diallo A, Eklu-Gadegkeku K, Agbonon A, Aklikokou K, Creppy E, Gbeassor M. Acute and subchronic (28-day) oral toxicity studies of hydroalcoholic extract of Lannea kerstingii Engl. and K. Krause (Anacardiaceae) stem bark. J Pharmacol Toxicol. 2010;5(7):343–9.
[50] Patel C, Dadhaniya P, Hingorani L, Soni M. Safety assessment of pomegranate fruit extract: acute and subchronic toxicity studies. Food Chem Toxicol. 2008;46(8):2728–35.
[51] Malik NS, Ahmad M, Minhas MU, Tulain R, Barkat K, Khalid I, et al. Chitosan/xanthan gum based hydrogels as potential carrier for an antiviral drug: fabrication, characterization, and safety evaluation. Front Chem. 2020;8:50.
[52] Pokharkar V, Dhar S, Bhumkar D, Mali V, Bodhankar S, Prasad B. Acute and subacute toxicity studies of chitosan reduced gold nanoparticles: a novel carrier for therapeutic agents. J Biomed Nanotechnol. 2009;5(3):233–9.
[53] Malonne H, Eeckman F, Fontaine D, Otto A, De Vos L, Moës A, et al. Preparation of poly (N-isopropylacrylamide) copolymers and preliminary assessment of their acute and subacute toxicity in mice. Eur J Pharm Biopharm. 2005;61(3):188–94.
[54] Cheaburu-Yilmaz CN, Atmaca K, Yilmaz O, Orhan H. Development, characterization, and evaluation of potential systemic toxicity of a novel oral melatonin formulation. Pharmaceutics. 2024;16(7):871.